First Approach for the Modelling of the Electric Field Surrounding a Piezoelectric Transformer in View of Plasma Generation

Clément Nadal, François Pigache, Yvan Lefèvre

HAL Id: hal-00779349
https://hal.science/hal-00779349

Submitted on 22 Jan 2013

First Approach for the Modelling of the Electric Field Surrounding a Piezoelectric Transformer in View of Plasma Generation

C. Nadal, F. Pigache, and Y. Lefevre

Université de Toulouse, INPT, UPS-CNRS-Laboratoire Plasma et Conversion d'Energie, ENSEEIHT, F-31071 Toulouse Cedex 7, France

This paper is about an open multi-physics modelling problem resulting from recent investigations into plasma generation by piezoelectric transformers. In this first approach, the electric field distribution surrounding the transformer is studied according to a weak coupling formulation. Electric potential distribution views obtained numerically are compared to real views of plasma generation observed experimentally.

Index Terms—**Electro-quasi static field problem, electrostatic field model, forced vibration analysis, modal analysis, numerical model, piezoelectric transformer, plasma generation.**

I. Introduction

PIEZOELECTRIC TRANSFORMERS (PT) are commonly used in numerous applications. Recently, several studies have underlined the capability to generate non-equilibrium plasma from the electrical potential on a piezoelectric element undergoing mechanical vibrations [1]. In this kind of application, the classical Rosen type transformer is used because of its high voltage step-up ratio. This structure consists of a single rectangular piece of piezoelectric ceramic material: the primary part is poled in the thickness direction whereas the secondary part is poled in the length direction as illustrated in Fig. 1. This device is driven by an AC voltage power supply applied to the primary part at a frequency close to the resonance frequency of a longitudinal mode.

Experimentally, it can be shown that plasma is generated at the secondary part of the transformer [1]. This plasma is mainly due to the electric field surrounding the transformer, and is issued from the electric potential distribution on the secondary part surface. Thus, in order to understand how the plasma is generated, the surrounding electric field distribution must be studied. This electric potential distribution produced on the surface of the secondary part is expressed analytically by a previous model developed in [2]. This analytical result is used to compute the distribution of the surrounding electrical field by means of a numerical model.

This paper is organised as follows. In Section II, it is first shown that Electro Quasi Static (EQS) assumptions can be made [3] and the problem can be reduced to an electrostatic problem. The PT analytical model is recalled in Section III and Section IV presents the numerical 2D electric field model. Finally, results showing the electric potential distributions are compared with real views of plasma glow discharges observed experimentally with different vibratory modes of the PT.
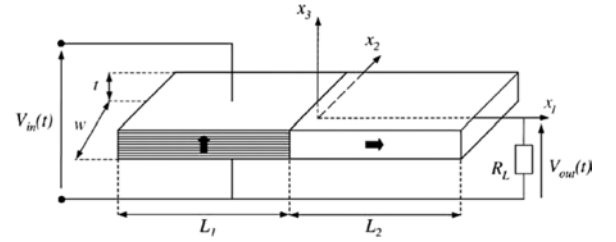

Fig. 1. Geometric parameters of a Rosen type PT.

II. Electro Quasi Static Field Approximations

The electric potential distribution on the surface of the PT secondary part creates a time varying electric field. In this first approach, we study the surrounding electric field under atmospheric pressure without the presence of plasma. The equations of electromagnetic field surrounding the transformer are as follows:

$$\mathbf{curl}E = -\frac{\partial \boldsymbol{B}}{\partial t} \tag{1}$$

$$\mathbf{curl}H = \boldsymbol{J} + \frac{\partial \boldsymbol{D}}{\partial t} \tag{2}$$

$$\mathrm{div}\boldsymbol{D} = 0 \tag{3}$$

$$\mathrm{div}\boldsymbol{B} = 0 \tag{4}$$

$$\boldsymbol{D} = \varepsilon_0 \boldsymbol{E} \tag{5}$$

$$\boldsymbol{B} = \mu_0 \boldsymbol{H} \tag{6}$$

where $\boldsymbol{H}$ is the magnetic field, $\boldsymbol{B}$ is the magnetic flux density, $\boldsymbol{E}$ is the electric field, $\boldsymbol{D}$ is the electric flux density, $\boldsymbol{J}$ is the current density, μ_0 is the magnetic permeability and ε_0 is the electric permittivity. Generally, in low frequency applications, one refers to the relaxation time which depends on the electric permittivity and the conductivity of the medium to neglect displacement current.

A Magneto Quasi Static (MQS) field approximation can then be done and the displacement current can be neglected. But here, the conductivity of free space is very low and the displacement current cannot be neglected. Equation (2) means that a magnetic field is created by the displacement and (1), so that this magnetic field may interact in return with the electric field. Equations (1) to (6) lead to the electromagnetic wave equation:

$$\mathbf{curl}(\mathbf{curl}E) + \sigma\mu_0\frac{\partial \boldsymbol{E}}{\partial t} + \varepsilon_0\mu_0\frac{\partial^2 \boldsymbol{E}}{\partial t^2} = 0 \tag{7}$$

TABLE II
STRUCTURAL PARAMETERS OF THE PT

ρ	Mass density	7600 kg.m^{-3}
s_{11}^E	Transversal compliance	1.256 10^{-11}m^{2}N^{-1}
s_{33}^E	Longitudinal compliance	1.61 10^{-11}m^{2}N^{-1}
d_{31}	Transversal piezoelectric factor	-1.329 10^{-10}mN^{-1}
d_{33}	Longitudinal piezoelectric factor	3.086 10^{-10}mN^{-1}
ε_{33}^T	Longitudinal permittivity	1454 ε_0 Fm^{-1}
k_{31}	Transversal coupling factor	0.330
k_{33}	Longitudinal coupling factor	0.678
Q_m	Mechanical quality factor	300

where σ is the conductivity of the medium. For the time harmonic electromagnetic field, this wave equation may be associated with the typical term:

$$(1/L)^2 - (\omega/c)^2 \qquad (8)$$

where L is the typical length scale of the problem, c the speed of light and ω the angular frequency of the field.

In our problem, the frequency of the AC power supply is less than 300 kHz [2]. So it yields:

$$c/\omega > 159 \text{ m} \qquad (9)$$

This value is very great in front of the typical length of a PT [2]:

$$L < 0.1 \text{ m} \qquad (10)$$

Thus, the wave propagation can be neglected and the problem can be reasonably considered as an Electro Quasi-Static (EQS) field problem, and dynamic term $\partial \boldsymbol{B}/\partial t$ can be neglected in (1) [3], [4].

By admitting there is no dissipation in the surrounding gas, the EQS problem can be considered as a succession of static field problems: at each time step the electric scalar potential is computed by solving a Laplace's equation where the electric scalar potential is imposed on the surface of the secondary part. For a given vibratory mode of the transformer, the electric potential on a point of the surface is synchronized by a sinusoidal time function with a magnitude depending on its location. As a consequence, for each vibratory mode, only one solution of the Laplace's equation is needed to know the distribution in space and the evolution in time of the electric field. Furthermore, previous studies have shown that the magnitude of electric potential can be considered as invariant along the width direction [2]. In first approximation, the problem can then be reduced to a 2D electrostatic field problem.

III. ANALYTICAL MODEL OF PIEZOELECTRIC TRANSFORMER

This section provides information about the studied PT and the employed analytical model [2].

A. Studied PT

Fig. 1 shows the geometric parameters of a classical Rosen Type PT: L_1 and L_2 are the lengths of the primary and secondary parts respectively, t the thickness and w the width.

The origin of the coordinate system is chosen at the centre of the interface between the primary and secondary parts. The primary part $-L_1 < x_1 < 0$ is made of m layers with e/m thickness. In the secondary part $0 < x_1 < L_2$, the output electrode at the end is connected at the load resistance R_L. In the present study, the secondary part is electrically open and the load is with

infinite value. The geometric and structural parameters are given in Tables I and II.

B. Analytical Model of Piezoelectricity in PT

According to the commonly made assumptions in PT studies and expressed in [2], PT undergoes an axial stress along the axis x_1 and is free of shear stress. The stress $\boldsymbol{S}$ and strain $\boldsymbol{T}$ tensors are reduced to one component along axis x_1:

$$\boldsymbol{T} = [T_1\, 0\, 0\, 0\, 0\, 0]^T \quad \boldsymbol{S} = [S_1\, 0\, 0\, 0\, 0\, 0]^T \qquad (11)$$

Each laminated layer of the primary part is supplied by a sinusoidal voltage, producing an electrical field oriented parallel to the axis x_3. Thus, the electric field and electric displacement vectors of the primary side are:

$$\boldsymbol{E_p} = [0\, 0\, E_3]^T \quad \boldsymbol{D_p} = [0\, 0\, D_3]^T \qquad (12)$$

This leads to the following reduced constitutive relationships between the electric field and mechanical tensors in the primary part:

$$T_1 = \bar{c}_{11}^E S_1 - \bar{e}_{31} E_3 \quad D_3 = \bar{e}_{31} S_1 + \bar{\varepsilon}_{33}^S E_3 \qquad (13)$$

where:

$$\bar{c}_{11}^E = \frac{1}{s_{11}^E} \quad \bar{e}_{31} = \frac{d_{31}}{s_{11}^E} \quad \bar{\varepsilon}_{33}^S = \varepsilon_{33}^T \left(1 - k_{31}^2\right) \qquad (14)$$

Concerning the secondary part, an ideal insulation medium is assumed. Hence the components of the electric field alongthe axes x_2 and x_3 are equal to zero. Thus, the electric field in the secondary part is parallel to the x_1 axis:

$$\bar{\boldsymbol{E_s}} = [E_1\, 0\, 0]^T \quad \boldsymbol{D_p} = [D_1\, 0\, 0]^T \qquad (15)$$

This leads to the following reduced constitutive relationships between the electric field and mechanical tensors in the secondary part:

$$T_1 = \bar{c}_{33}^D S_1 - \bar{h}_{33} D_1 \quad E_1 = -\bar{h}_{33} S_1 + \bar{\beta}_{33}^S D_1 \qquad (16)$$

where

$$\bar{c}_{33}^D = \frac{1}{s_{33}^E \left(1 - k_{33}^2\right)} \quad \bar{h}_{33} = \frac{k_{33}^2}{d_{33} \left(1 - k_{33}^2\right)} \quad \bar{\beta}_{33}^S = \frac{1}{\varepsilon_{33}^T \left(1 - k_{33}^2\right)} \qquad (17)$$

The analytical model of PT has been presented in [2]. This multimodal general approach is based on Hamilton's principle. Finally, the application of the modal superposition method leads
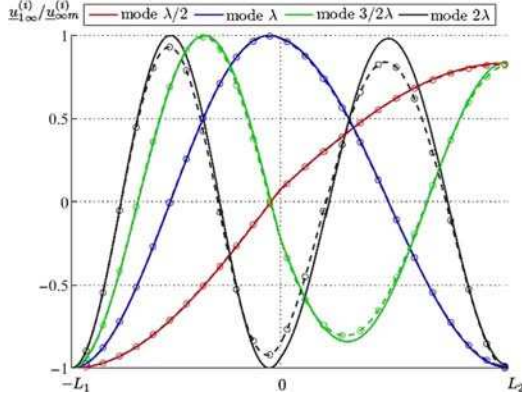
Fig. 2. First four mechanical mode wave shapes obtained by the analytical model (solid lines) and ANSYS (dashed lines).
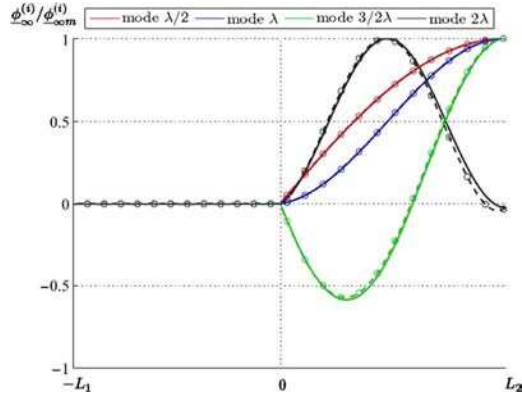

Fig. 3. Normalized electric potential distribution corresponding to the first 4 mode waveshapes obtained by the analytical model (solid lines) and ANSYS (dashed lines).

TABLE III
MODAL FREQUENCIES OBTAINED BY ANALYTICAL MODEL, ANSYS AND MEASUREMENTS

	Analytical model	ANSYS	Measurements
Mode $\lambda/2$	70.5 kHz	70.6 kHz	68.9 kHz
Mode λ	142.5 kHz	141.2 kHz	138.7 kHz
Mode $3\lambda/2$	211.7 kHz	206.5 kHz	206.7 kHz
Mode 2λ	284.9 kHz	265.3 kHz	266kHz

to proceeding to a modal analysis relying on forced vibration analysis [5].

C. Modal Analysis

The first four longitudinal vibratory modes have been calculated by this analytical model and compared to the results of modal analysis performed with *ANSYS Academic Research, Release 11.0*. An infinite value of the resistance R_L is taken. Fig. 2 shows the four modal wave shapes along x_1 obtained analytically and numerically. Fig. 3 shows the corresponding normalized electric potential distribution.

These results show that in spite of the 1D model approximation, the analytical model calculates correctly the mechanical mode shapes and their corresponding normalized electric potential distributions. Table III gives the resonant frequencies analytically, numerically and experimentally obtained. It shows a good accuracy of theoretical results with experiments.
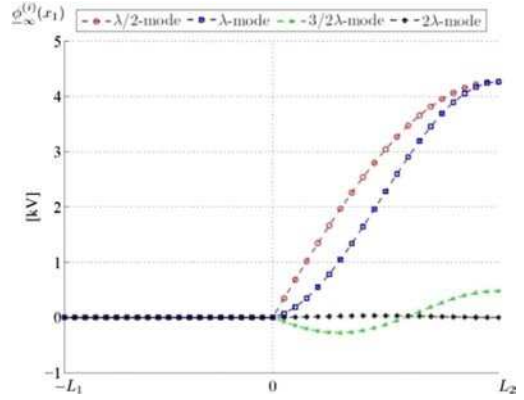

Fig. 4. Distributions of the electric potential along the x-axis when vibration is forced with frequency supply near each modal frequency.

D. Forced Vibration Analysis

After calculating the mode wave shapes, forced vibration can be calculated. In this case, the electric potential at the primary part is imposed equal to the sinusoidal supply voltage $V_{in}(t)$ (Fig. 1). Moreover, the secondary part is still electrically open. In order to avoid a theoretical infinite value of the calculated potential, and displacement when the supply frequency is equal to the modal frequency, mechanical losses have to be taken into account. Therefore, some parameters of the piezoelectric model in (13) and (16) are usually replaced by complex numbers:

$$\hat{c}_{11}^E = \bar{c}_{11}^E \left(1 + \frac{j}{Q_m}\right) \quad \hat{c}_{33}^D = \bar{c}_{33}^D \left(1 + \frac{j}{Q_m}\right) \qquad (18)$$

where Q_m is the mechanical factor given in Table II.

The electric potential distributions along axis x_1 for supply frequencies close to the modal ones have been obtained by the analytical model and are illustrated in Fig. 4. It is worth noting that the electric potential corresponding to the 2λ mode is very low compared to the others, and it cannot be sufficient to produce a glow discharge.

IV. NUMERICAL MODEL OF THE ELECTRIC FIELD

In order to solve the steady state problem of electrical potential surrounding the piezoelectric device, the Finite Difference Method (FDM) is applied because it can be implemented easily for this first approach [6]. Obviously, this model is a weak coupling formulation relying on the previous analytical model and a numerical 2D model for the electric field equations.

Fig. 5 shows the rectangular study domain D in which the upper-half part of a Rosen type transformer is considered. (Ω), (Ω_{in}), (Ω_{out}) and (Γ_D) are the surrounding medium, the primary and the secondary parts and the Dirichlet boundaries, respectively, where the electrical potential is vanishing. The Rosen type transformer is supposed to be surrounded by a free electric charge air with vacuum permittivity ε_0. The primary part is considered as a dielectric medium with a high relative permittivity ($\approx$1000). A z-invariance and x-axis symmetry are supposed.

Consequently, the electrical potential produced on the secondary side follows the boundary problem shown in Fig. 5, where Δ is the Laplace operator and and ϕ_{PT} is the electrical potential calculated by the analytical model (Fig. 4). In order to discretize this elliptic PDE, a 5-point instead of a 9-point stencils method is sufficient.
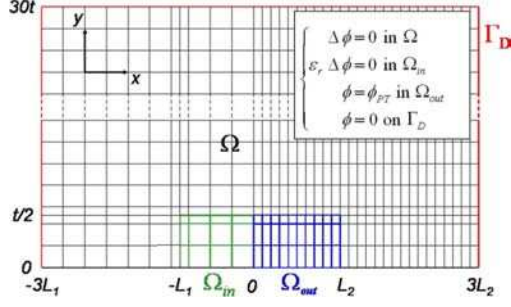
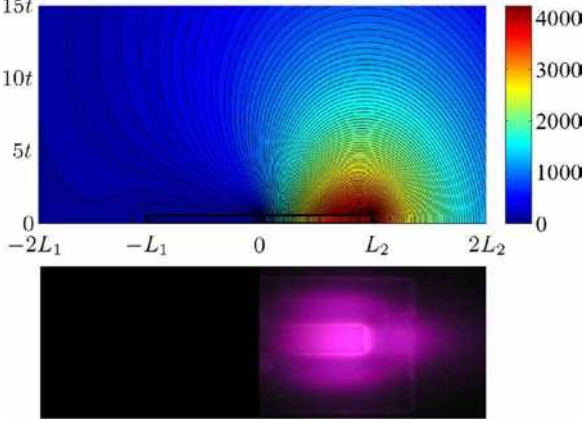Fig. 5. Domain definition of the numerical problem of the electrical potential generated by a Rosen type PT.

Fig. 6. Top: cross-section view of numerical electrical potential (V) distribution ($\lambda/2$-mode); bottom: front view of experimental glow discharge ($\lambda/2$-mode).

Fig. 7. Top: cross-section view of numerical electrical potential (V) distribution (λ-mode); bottom: front view of experimental glow discharge (λ-mode).

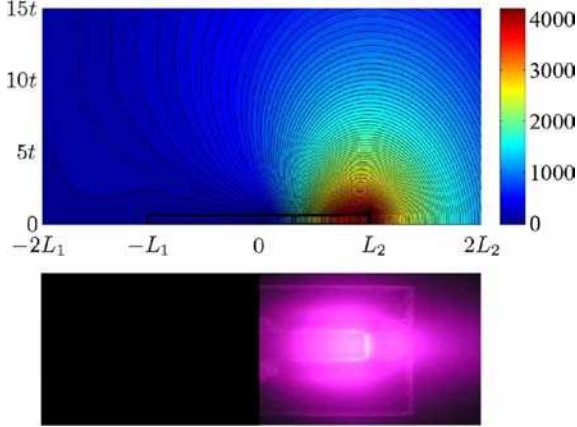## V. RESULTS

For each resonant longitudinal vibratory mode, the electric potential distribution calculated by the analytical model of PT (Fig. 4) is applied on the definitiondomain of (Ω_{out}). Cross-sectional views of the electric potential in the domain (Ω) obtained for each of the first three modes are shown at the top of Fig. 6, Fig. 7 and Fig. 8. These views can be compared with front views of the experimentally observed glow discharges at the bottom of Fig. 6, Fig. 7 and Fig. 8. Table IV gives the experimental conditions to generate plasma glow discharges for the first three modes of vibration. It can be noticed that the frequencies are very close to the modal frequencies given in Table III.

The visual similarity between the high gradient electric potential areas and the luminescent areas for each mode is note-
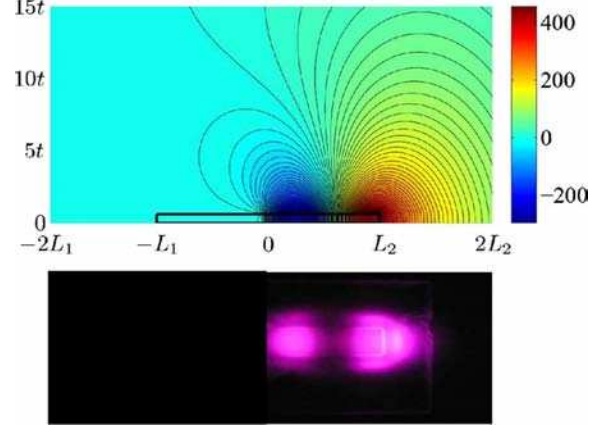

Fig. 8. Top: cross-section view of numerical electrical potential (V) distribution ($3/2\lambda$-mode); bottom: front view of experimental glow discharge ($3/2\lambda$-mode).

TABLE IV
EXPERIMENTAL CONDITIONS OF PLASMA GLOW DISCHARGES FOR THE FIRST THREE LONGITUDINAL VIBRATORY MODES

Mode	Pressure[mbar]	V_{in} [V]	Supply frequency [kHz]
$\lambda/2$	2.4	1.8	70.80
λ	2.4	1.8	140.9
$3\lambda/2$	2.4	1.8	207.6

worthy. Moreover, there is no visible glow discharge for the 2λ-mode, as suggested theoretically by the weak field obtained from the numerical study and using results of Fig. 4.

VI. CONCLUSION

With the objective to move the piezoelectric and plasma domains closer, this preliminary study has concerned the weak coupling of piezoelectricity and the surrounding electric field. Results obtained are very interesting and encouraging. In light of recent experimental observations, which have shown a significant influence of glow discharge on the electric behaviour of the PT, it clearly appears that the coupling relation is stronger than suggested in this paper. The modelling of this open multiphysics problem will require a more accurate study, linking the electric field equations with the local equations of the piezoelectricity and cold plasma equations.

REFERENCES

[1] K. Teranishi, H. Itoh, and S. Suzuki, "Dynamic behavior of light emissions generated by piezoelectric transformers," *IEEE Trans. Plasma Sci.*, vol. 30, no. 2, pp. 122–123, Feb. 2002.

[2] C. Nadal and F. Pigache, "Multimodal electromechanical model of piezoelectric transformers by Hamilton's principle," *IEEE Trans. Ultrason., Ferroelectr. Freq. Contr.*, vol. 56, no. 11, pp. 2530–2543, Nov. 2009, 10.1109/TUFFC.2009.1340.

[3] Z. Badics, "Charge density-scalar potential formulation for adaptive time-integrationof nonlinear electroquasistatic problems," *IEEE Trans. Magn.*, vol. 47, no. 5, pp. 1338–1341, May 2011.

[4] T. Steinmetz, M. Helias, G. Wimmer, L. Fichte, and M. Clemens, "Electro-quasistatic field simulations based on a discrete electromagnetism formulation," *IEEE Trans. Magn.*, vol. 42, no. 4, pp. 755–758, Apr. 2006.

[5] H. Javadi, Y. Lefevre, S. Clenet, and M. Lajoie-Mazenc, "Electro-magneto-mechanical characterizations of the vibration of magnetic origin OE electrical machines," *IEEE Trans. Magn.*, vol. 31, no. 3, pp. 1892–1895, May 1995.

[6] C. F. Campbell and R. J. Weber, "Two-dimensional finite difference method for the analysis of piezoelectric devices," in *IEEE Proc. Ultrasonics Symp.*, Oct. 1992, vol. 1, pp. 477–481.